Original Article

http://dx.doi.org/10.3348/kjr.2011.12.6.671
pISSN 1229-6929 · eISSN 2005-8330
Korean J Radiol 2011;12(6):671-678

Korean Journal of Radiology
KJR

Lymphomatoid Granulomatosis: CT and FDG-PET Findings

Jonathan H. Chung, MD[1], Carol C. Wu, MD[2], Matthew D. Gilman, MD[2], Edwin L. Palmer, MD[2], Robert P. Hasserjian, MD[3], Jo-Anne O. Shepard, MD[2]

[1]Institute of Advanced Biomedical Imaging, National Jewish Health, Denver, CO 80206, USA; Departments of [2]Radiology and [3]Pathology, Massachusetts General Hospital, Boston, MA 02114, USA

Objective: Lymphomatoid granulomatosis (LG) is a rare, aggressive extranodal Epstein-Barr virus (EBV)-positive B-cell lymphoproliferative disease. The purpose of our study was to analyze the CT and fluorodeoxyglucose positron emission tomography (FDG-PET) findings of pulmonary LG.

Materials and Methods: Between 2000 and 2009, four patients with pathologically proven pulmonary LG and chest CT were identified. Two of these patients also had FDG-PET. Imaging features of LG on CT and PET were reviewed.

Results: Pulmonary nodules or masses with peribronchovascular, subpleural, and lower lung zonal preponderance were present in all patients. Central low attenuation (4 of 4 patients), ground-glass halo (3 of 4 patients), and peripheral enhancement (4 of 4 patients) were observed in these nodules and masses. An air-bronchogram and cavitation were seen in three of four patients. FDG-PET scans demonstrated avid FDG uptake in the pulmonary nodules and masses.

Conclusion: Pulmonary LG presents with nodules and masses with a lymphatic distribution, as would be expected for a lymphoproliferative disease. However, central low attenuation, ground-glass halo and peripheral enhancement of the nodules/masses are likely related to the angioinvasive nature of this disease. Peripheral enhancement and ground-glass halo, in particular, are valuable characteristic not previously reported that can help radiologists suggest the diagnosis of pulmonary LG.

Index terms: *Lymphomatoid granulomatosis; Cavitation; Pulmonary nodules; Pulmonary masses; Halo sign; Air-bronchogram sign*

INTRODUCTION

Lymphomatoid granulomatosis (LG) is a rare, aggressive, angiodestructive, extranodal Epstein-Barr virus (EBV)-positive B-cell lymphoproliferative disease with reactive T-cells (1). Reactive T-cells often predominate in the background, and therefore, LG was first thought to be a T-cell disorder. First described in 1972, LG was initially categorized as a subset of pulmonary granulomatous vasculitis (2). Prior names for LG include angiocentric lymphoma and angiocentric immunoproliferative lesion, which reflect the vascular-centered morphology of abnormal cells on pathology.

Though the imaging appearance of LG on chest radiography has been described in multiple series, the CT appearance of pulmonary LG has not been well delineated (3-6). To our knowledge, only one other cases series has

Received May 21, 2011; accepted after revision July 22, 2011.
Jonathan H. Chung, MD receives salary support from Siemens AG and the NIH.

Corresponding author: Jonathan H. Chung, MD, Institute of Advanced Biomedical Imaging, National Jewish Health, 1400 Jackson St., Denver, CO 80206, USA.
• Tel: (1619) 300-0335 • Fax: (1303) 270-2219
• E-mail: chungj@njhealth.org

studied the CT appearance of pulmonary LG (7). Most descriptions of CT and fluorodeoxyglucose positron emission tomography (FDG-PET) appearance of LG were presented in isolated case reports (8-10). The purpose of our study was to analyze the CT and FDG-PET findings in patients with pathologically proven pulmonary LG.

MATERIALS AND METHODS

A retrospective review of patient data and of radiological studies was approved by our Institutional Review Board. No patient consent was required for this Health Insurance Portability and Accountability Act (HIPAA)-compliant study. Between 2000 and 2009, four patients with pathologically proven pulmonary LG and chest CT scans within two weeks of pathological diagnosis were identified by a database search of the radiology and pathology reports at our institution. Medical records were reviewed to determine patient age, gender, initial presentation, medical history, grade of LG, means of tissue diagnosis, and treatment regimen.

Tissue diagnosis and grading of cases was based on the 2008 WHO classification (11). In three of the patients, the diagnosis was made based on the surgical wedge resection of pulmonary nodules and masses. In one of the patients, the diagnosis was initially made by a liver biopsy, and pulmonary involvement was later confirmed at the autopsy.

Two of the three patients also underwent FDG-PET scans prior to initiation of treatment. In one of these two patients, the initial PET scan was performed within three weeks of the chest CT. The follow-up PET of this patient and all three of the PET studies of the other patient were performed by concurrent CT.

CT scans of the chest from 2001 to 2009 were performed on various multi-detector CT scanners. The CT parameters ranged from 120-140 kVp, 260 to 432 mA, and 2.5 to 5 mm slice thickness reconstruction; two of these patients had CT scans performed with automatic tube current modulation. All scans were performed with IV contrast. Images were reviewed in the lung, soft tissue, and bone windows. PET scans were performed 60 minutes after injection of approximately 15 mCi of F-18 FDG; tomographic images of the body from the neck to the proximal thigh were acquired in 3D mode on either a Siemens HR+ PET scanner, Siemens Biograph 64 (Siemens Medical Systems, Erlangen, Germany), or GE Discovery 64 PET/CT scanner (GE Medical Systems, Milwaukee, WI). Standardized uptake values (SUV) were determined as the maximum value within the lung tumors, as a function of body weight. PET and CT images were displayed and registered on a Siemens Multimodality Workstation using True-D imaging software.

CT scans were reviewed retrospectively by two board-certified, fellowship-trained chest radiologists who were aware of the diagnosis of LG in these patients. Disagreements were resolved by consensus. Data recorded from the CT scans included the number and size range of the lung nodules or masses. The presence of cavitation or central air density, central low attenuation defined as < 20 Hounsfield unit, air bronchograms, ground-glass halo, and peripheral enhancement of the nodule or masses was recorded. Other findings such as ground-glass opacities, interlobular and intralobular septal thickening, consolidation, lymphadenopathy, and pleural effusions were also recorded. The axial (peribronchovascular, subpleural, or random) and craniocaudal (upper, mid, lower) distribution of the disease was documented. Follow up CT scans were also reviewed

Table 1. Demographics, Clinical Presentation, and Disease Course

Patient	Age	Gender	Presentation	Treatment	Disease Course
1	51	Male	Left pleuritic chest pain	R-CHOP, methotrexate	Responded to treatment, in remission 1 1/2 years after initial diagnosis
2	58	Male	Rash, vision changes (pulmonary findings incidental on CXR)	R-CHOP	Responded to treatment, developed pancreatic cancer with liver metastases
3	39	Male	Cough, dyspnea	Rituximab	Progression, died of pneumonia and respiratory failure
4	60	Male	Fever, weight loss, night sweat	Interferon followed by EPOCH, then Rituximab. stem cell transplant	Progression, died of pneumonia and respiratory failure

Note.— CXR = chest X-ray, EPOCH = Etoposide, Prednisone, Vincristine (Oncovin), Cyclophosphamide, Doxorubicin (Hydroxydoxorubicin), R-CHOP = Rituximab-Cyclophosphamide, Doxorubicin (Hydroxydoxorubicin), Vincristine (Oncovin), Prednisone

Korean Journal of Radiology
KJR

to determine if there was a response to treatment. In cases where FDG-PET was performed, activity within the nodules was assessed in conjunction with a board certified, fellowship-trained nuclear medicine physician. Because of the small number of patients in the study, statistical analyses were not warranted.

RESULTS

Patient demographics, clinical presentations, and disease course are as summarized in Table 1. The mean age of the patients was 52 year old. All four patients were men. No affected patients were immunocompromised. Patient 3 had a history of congenital deafness. Clinical presentation ranged from relatively mild respiratory symptoms to highly symptomatic systemic manifestations. All patients in our series were treated with chemotherapy. Two of the patients responded to chemotherapy, whereas two of the patients had progressive disease.

The pathological diagnosis of LG was made based on a surgical biopsy specimen. Three of the patients had CT-guided percutaneous needle aspirate/biopsy of the lung nodules/masses, which did not result in the specific diagnosis of LG prior to surgical biopsy. Patient 1 had a histological grade of 2, patient 2 had a histological grade of 3, and patients 3 and 4 had histological grades of 1 which eventually progressed to grade 3.

The main findings on chest CT are as summarized in Table 2. Selected pertinent images of each patient are included in Figures 1-4. Pulmonary nodules and masses seen in all of the patients, multiple nodules and masses seen in three of the patients, and solitary nodules and masses in one of the patients. The nodules and masses were lower-lobe predominant with a peribronchovascular and/or subpleural distribution in the axial plane.

All four of the patients had nodules or masses that demonstrated peripheral enhancement, central low attenuation, and ground-glass halo. Air-bronchograms were present in three patients, whereas cavitary nodules/masses were present in two patients.

Avid FDG uptake was present in both patients (patient 1 and 2) who had FDG-PET (Figs. 1, 2). Nodules and masses larger than 2 cm in both patients demonstrated a paucity of central FDG uptake. For patient 1, the maximum SUV within the pulmonary nodules/masses at baseline was 7.3; whereas, the maximum SUV within pulmonary nodules/masses on follow up scan (58 days later) had decreased to 3.5 post

Table 2. Summary of Chest CT Findings

Patient	Number of Nodules/ Masses	Size of Nodules/ Masses	Peripheral Enhancement	Central Low Density	Ground-Glass Halo	Cavitation (central air)	Air -Bronchogram	Cranio-Caudal Distribution	Axial Distribution	Other Findings
1	8	8-55 mm	All nodules and masses	All nodules and masses	All nodules and masses	1/8 nodules and masses	3/8 nodules and masses	Lower lobe predominant	PBV and subpleural	Small pleural effusion, left chest wall mass, liver lesions
2	24	4-57 mm	17/24 of nodules and masses	21/24 of nodules and masses	17/24 of nodules and masses	2/24 nodules and masses	8/24 of nodules and masses	Lower lobe predominant	PBV and subpleural	PBV groundglass opacities and nodules mildly enlarged lymph nodes
3	> 40	4-66 mm	32/> 40 nodules and masses	All nodules and masses	28/> 40 nodules and masses	5/> 40 nodules and masses	8/> 40 of nodules and masses	Lower lobe predominant	PBV and subpleural	Small pleural effusion
4	1	24 mm	Yes	Yes	No	No	No	Lower lobe	Subpleural	Liver lesions

Note.— PBV = peribronchovascular

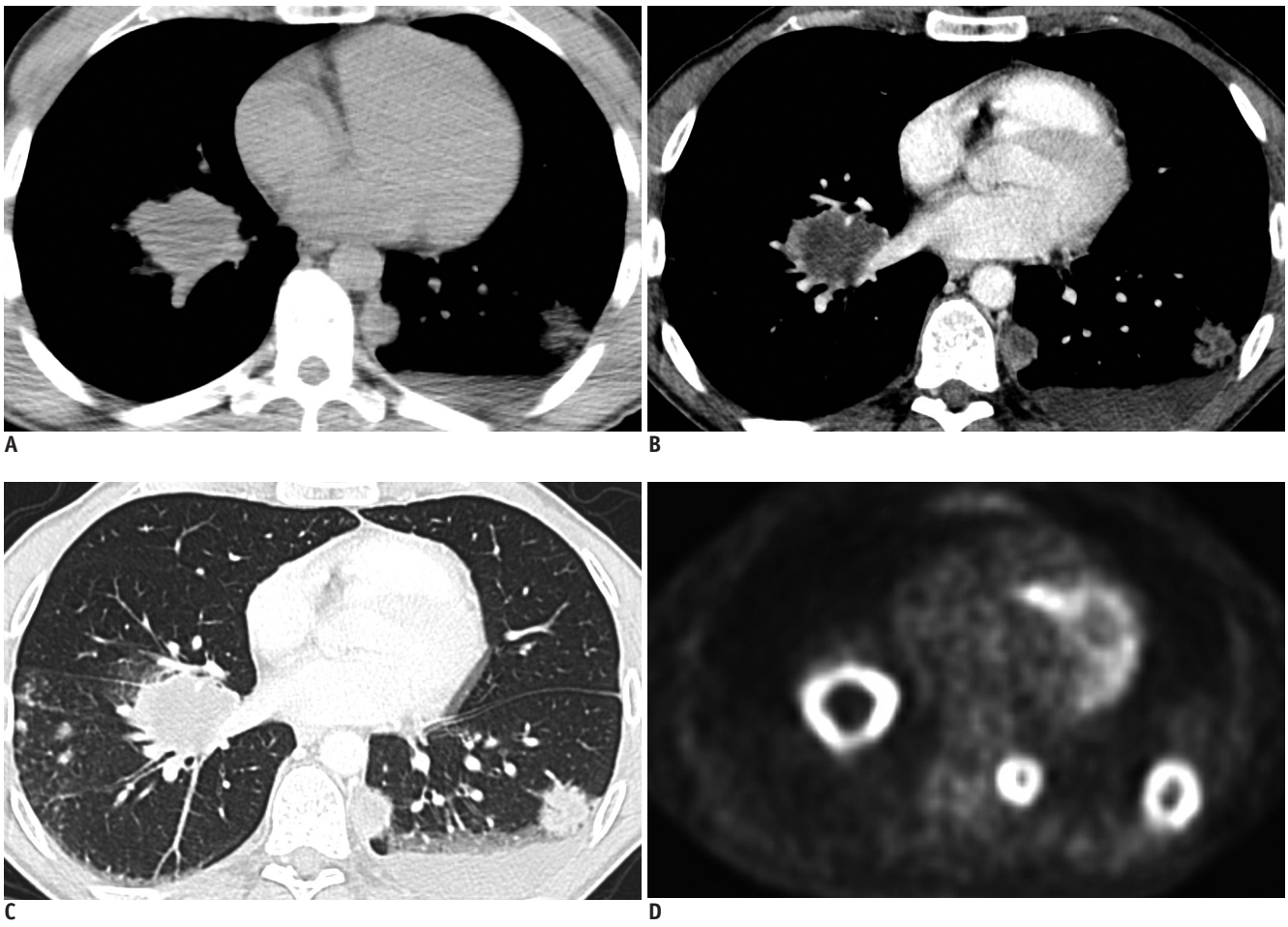

Fig. 1. Chest CT and FDG-PET images of patient 1.
A. Axial pre-contrast CT image demonstrates peribronchovascular pulmonary nodules/mass and small left pleural effusion. **B.** Axial post-contrast CT image shows peripheral enhancement and central low attenuation of nodules/mass. **C.** Axial CT image in lung window shows subtle ground-glass halo of two left lower lobe nodules as well as ground-glass opacity in anterolateral aspect of right lower lobe mass. Air-bronchogram is noted in lateral left lower lobe nodule. Small peribronchovascular nodules are noted in right lower lobe. **D.** Axial FDG-PET image demonstrates peripheral FDG uptake in pulmonary nodules/mass.

treatment. For patient 2, the maximum SUV within the pulmonary nodules/masses at baseline was 10.8; whereas, the maximum SUV within the pulmonary nodules/masses on post-treatment scan (39 days later) had decreased to 4.3. FDG uptake was seen in the left chest wall mass and hepatic lesions of patient 1. No FDG avidity was present in mediastinal or hilar lymph nodes in either patient; even though patient 2 had mildly enlarged mediastinal nodes.

DISCUSSION

Lymphomatoid granulomatosis is an angiodestructive EBV-positive lymphoproliferative disease, which clinically and histologically, can mimic pulmonary lymphoma and Wegener granulomatosis (WG). Affected patients often present with non-specific symptoms such as cough, shortness of breath, chest pain, and B symptoms (fever, weight loss, malaise) (2), as in our series. LG primarily affects the pulmonary system; however, it can also affect the skin (39% of cases), the nervous system (30% of cases), kidneys, liver, and GI tract (12). In our series, two of the four patients had hepatic involvement. In addition, affected patients are often immunocompromised (Wiskott-Aldrich syndrome, human immunodeficiency virus [HIV], or lymphoma) though none of them were immunocompromised in our study. Prognosis is poor with up to two of three of patients dying within the first year of diagnosis; typically due to secondary infection (12).

Gross pathological specimens are significant for centrally necrotic nodules. Angiodestructive and angioinvasive polymorphic lymphoid infiltration is common, and is composed mainly of lymphocytes (mainly reactive T-cells,

Korean Journal of Radiology
KJR

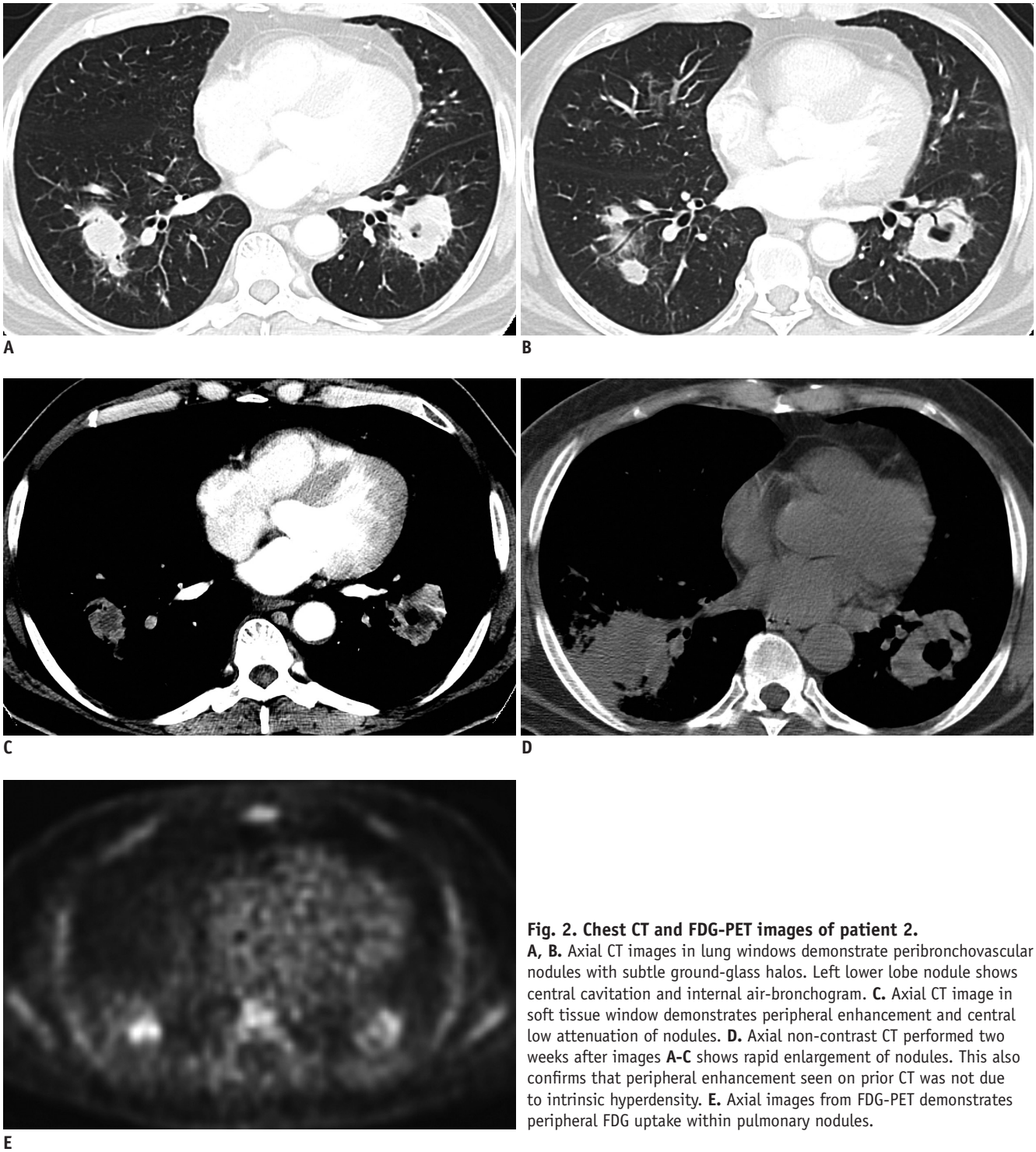

Fig. 2. Chest CT and FDG-PET images of patient 2.
A, B. Axial CT images in lung windows demonstrate peribronchovascular nodules with subtle ground-glass halos. Left lower lobe nodule shows central cavitation and internal air-bronchogram. **C.** Axial CT image in soft tissue window demonstrates peripheral enhancement and central low attenuation of nodules. **D.** Axial non-contrast CT performed two weeks after images **A-C** shows rapid enlargement of nodules. This also confirms that peripheral enhancement seen on prior CT was not due to intrinsic hyperdensity. **E.** Axial images from FDG-PET demonstrates peripheral FDG uptake within pulmonary nodules.

with varying numbers of large atypical B-cells), plasma cells, and histiocytes. The relative number of the neoplastic large B-cells and degree of cytological atypia are the basis for the 3-tier grading system in LG. Histological grading of LG has important ramifications for management and prognosis (13). Grade 1 lesions are composed of a polymorphous lymphoid infiltrate with few large neoplastic B cells and without necrosis. Grade 2 lesions are composed of more frequent large neoplastic B cells in a polymorphic background with some areas of necrosis. Grade 3 lesions are composed of numerous large neoplastic B cells that form sheets with extensive necrosis and is treated as a large B-cell lymphoma (13). Our patients had varying histological grades; ranging from 1-3. Two patients showed grade 1

A B

Fig. 3. Contrast-enhanced chest CT of patient 3.
A. Axial image in soft tissue window demonstrates multiple pulmonary nodules and masses with peripheral enhancement and central low attenuation. Mass in right lower lobe is cavitary. **B.** Axial image in lung window demonstrates presence of air-bronchogram and ground-glass halo (arrows) of some nodules. Nodules and masses are distributed along bronchovascular bundle and in subpleural region.

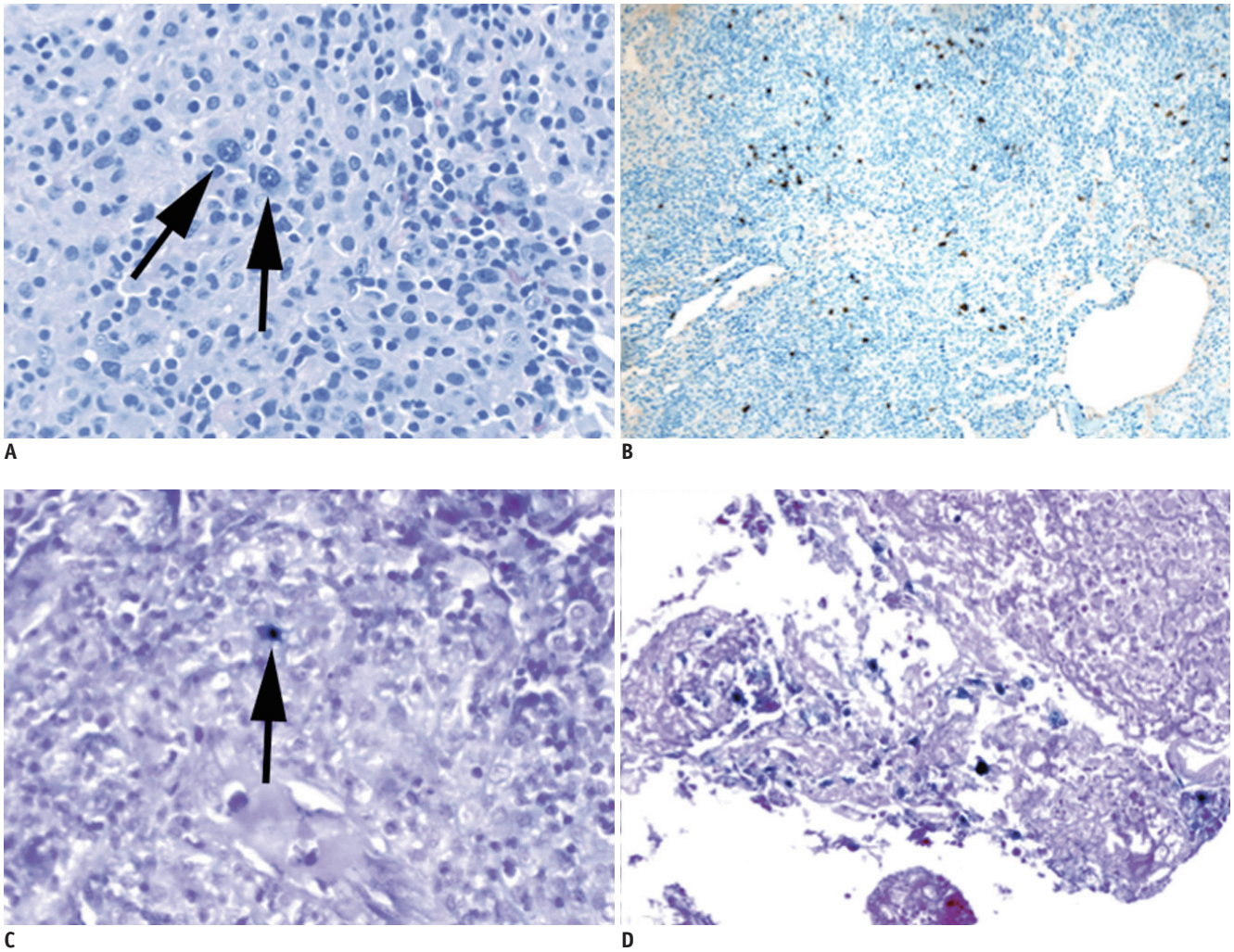

A B C D

Fig. 4. Pathology of lymphomatoid granulomatosis of patient 3.
A. Initial biopsy showed grade 1 histology, with only isolated large neoplastic cells (arrows) in predominant background of small lymphocytes (Hematoxylin & Eosin staining). **B, C.** Sparse neoplastic cells are positive for B-cell marker CD20 (**B,** immunostain for CD20) and for Epstein-Barr virus (EBV) (arrow) (**C,** Epstein-Barr encoded RNA in situ hybridization). **D.** In subsequent biopsy, EBV-positive neoplastic cells are more frequent, concurrent with progression to grade 3 histology (Epstein-Barr encoded RNA in situ hybridization).

Korean Journal of Radiology
KJR

histology, which eventually progressed to grade 3 histology.

Many of the findings in our study are similar to those previously reported in the radiology literature (3, 4, 7-9, 14). As in other studies, our patients had pulmonary nodules or masses, with a lower lung preponderance. In addition, most of the cases in our series demonstrated a peribronchovascular preponderance of pulmonary nodules as described in the only other series studying the CT appearance of pulmonary LG (7). The propensity of pulmonary LG in our study to affect peribronchovascular and subpleural regions, which corresponds to a perilymphatic distribution, is as expected for a lymphoproliferative disorder. Internal air bronchograms in nodules and masses, seen in three of our patients with LG, also has also been described previously (7). An air-bronchogram has also been described in the setting of infection, with bronchogenic lung cancer (typically bronchioloalveolar cell carcinoma) (8, 9, 14, 15), lymphoma, and WG (16-19). A low attenuation center and central cavitation of nodules/masses, seen in our study, has also been previously reported (3), and correspond to the histological findings of central necrosis.

To our knowledge, the ground-glass halo and peripheral enhancement of pulmonary nodules and masses have not been specifically described in LG. Initially described in angioinvasive aspergillosis (17), ground-glass halo was thought to represent a specific finding. Many other conditions have now been associated with this CT manifestation (20). Pathologically, the surrounding halo of ground-glass opacities may represent hemorrhage, inflammation, or tumor spread. Three out of four patients in our series had nodules or masses demonstrating the halo sign. Given LG's angioinvasive nature, the areas of ground-glass surrounding nodules or masses likely represent hemorrhage. Peripheral enhancement of the nodules/masses was seen in all of the patients in our study in the majority of nodules and masses. The peripheral enhancement is also likely related to the angio-invasive and angio-destructive nature of the LG.

A high index of suspicion for LG based on the combination of CT findings may have significant implications in further work-up and management of patients. In our series, the final diagnosis of LG in all four cases was made based on a surgical biopsy or autopsy specimen. Three of four patients underwent a CT-guided core needle biopsy, which did not yield the specific diagnosis of LG, possibly due to largely necrotic centers of these lesions. In addition, suspicion based on CT findings can also help guide and prompt

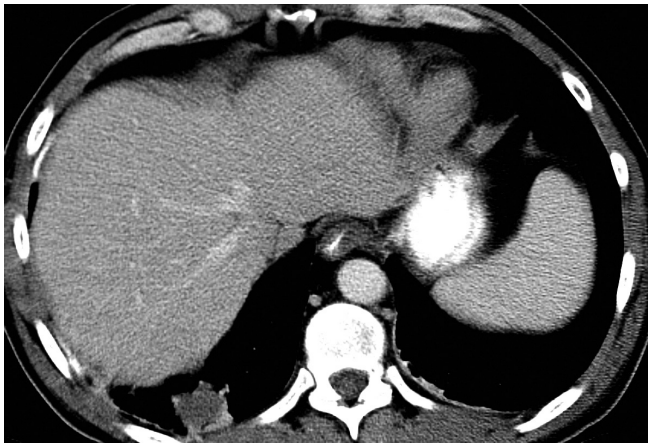

Fig. 5. Contrast-enhanced chest CT of patient 4. Axial image demonstrates solitary nodule in posterior costophrenic right lower lobe with peripheral enhancement and central low attenuation.

specific immuno-staining for B-cell lymphocyte markers and *in situ* hybridization of EBV encoded RNA (EBER) to aid the diagnosis of this rare entity (Fig. 5).

All previously described cases of FDG PET in the setting of LG have shown increased uptake in pulmonary nodules and masses (8, 9, 14, 15). Only in one case report is there a suggestion of peripheral uptake in the walls of the cavitary pulmonary lesions (14). Nodules and masses larger than 2 cm in our study demonstrated the paucity of central FDG uptake, consistent with the histological finding of central necrosis. After treatment, the maximum SUV within the pulmonary nodules/masses decreased, suggesting a response to treatment.

Coarse linear opacities described by Lee et al. (7) were not a major finding in our series. Though never explicitly stated, the linear opacities in their series may have represented a healing phase of nodules and masses as coarse linear opacities that became more prominent with the treatment of pulmonary LG in one of their patients. The CT scans included in our study were performed within two weeks of pathological diagnosis; Lee et al. (7) may have been more inclusive in the CT scans they included if the timing of imaging relative to pathological diagnosis in their series had been reported. Also, the reverse halo sign (central focus of ground-glass opacity surrounded by a rim of consolidation) has also been described in the setting of pulmonary LG (21). None of our cases demonstrated this unusual finding.

Pulmonary LG shares many of the same imaging manifestations of more common pulmonary conditions such as WG and pulmonary lymphoma, and should be considered when these more common diagnoses have

been excluded. This is especially true in patients with underlying immunosuppression (Wiskott-Aldrich syndrome, HIV, or lymphoma) as well as in patients with concomitant brain lesions. The combination of lower lung predominant peribronchovascular or subpleural pulmonary nodules and masses with central low attenuation, ground-glass halo, and peripheral enhancement should prompt consideration of this rare entity.

Acknowledgments

Primary research performed in the Department of Radiology, Massachusetts General Hospital.

REFERENCES

1. Guinee D Jr, Jaffe E, Kingma D, Fishback N, Wallberg K, Krishnan J, et al. Pulmonary lymphomatoid granulomatosis. Evidence for a proliferation of Epstein-Barr virus infected B-lymphocytes with a prominent T-cell component and vasculitis. *Am J Surg Pathol* 1994;18:753-764
2. Liebow AA, Carrington CR, Friedman PJ. Lymphomatoid granulomatosis. *Hum Pathol* 1972;3:457-558
3. Dee PM, Arora NS, Innes DJ Jr. The pulmonary manifestations of lymphomatoid granulomatosis. *Radiology* 1982;143:613-618
4. Hicken P, Dobie JC, Frew E. The radiology of lymphomatoid granulomatosis in the lung. *Clin Radiol* 1979;30:661-664
5. Wechsler RJ, Steiner RM, Israel HL, Patchefsky AS. Chest radiograph in lymphomatoid granulomatosis: comparison with Wegener granulomatosis. *AJR Am J Roentgenol* 1984;142:79-83
6. Prenovault JM, Weisbrod GL, Herman SJ. Lymphomatoid granulomatosis: a review of 12 cases. *Can Assoc Radiol J* 1988;39:263-266
7. Lee JS, Tuder R, Lynch DA. Lymphomatoid granulomatosis: radiologic features and pathologic correlations. *AJR Am J Roentgenol* 2000;175:1335-1339
8. Arai H, Oshiro H, Yamanaka S, Yukawa N, Wada N, Rino Y, et al. Grade I lymphomatoid granulomatosis with increased uptake of [18F] fluorodeoxyglucose in positron emission tomography: a case report. *J Clin Exp Hematop* 2009;49:39-44
9. Roarke MC, Nguyen BD. PET/CT characterization and monitoring of disease activity in lymphomatoid granulomatosis. *Clin Nucl Med* 2007;32:258-259
10. Rossi G, Marchioni A, Guicciardi N, Bertolini F, Valli R, Cavazza A. A rare cause of fever and PET-positive nodules in the lungs. *Clin Respir J* 2009;3:118-120
11. Pittaluga S, Jaffe ES. *Lymphomatoid granulomatosis*. In: Swerdlow SH, Campo E, Harris NL, Jaffe ES, Pileri SA, Stein H, eds. *WHO classification of tumours of haematopoietic and lymphoid tissues*. Lyon: IARC Press, 2008:247-249
12. Katzenstein AL, Carrington CB, Liebow AA. Lymphomatoid granulomatosis: a clinicopathologic study of 152 cases. *Cancer* 1979;43:360-373
13. Guinee DG Jr, Perkins SL, Travis WD, Holden JA, Tripp SR, Koss MN. Proliferation and cellular phenotype in lymphomatoid granulomatosis: implications of a higher proliferation index in B cells. *Am J Surg Pathol* 1998;22:1093-1100
14. Yamauchi Y, Yoshizawa A, Kudo K, Okuwaki H, Niino H, Morita T. [A case of lymphomatoid granulomatosis with multiple thin-walled cavities]. *Nihon Kokyuki Gakkai Zasshi* 2002;40:292-298
15. Vahid B, Salerno DA, Marik PE. Lymphomatoid granulomatosis: a rare cause of multiple pulmonary nodules. *Respir Care* 2008;53:1227-1229
16. Collins J. CT signs and patterns of lung disease. *Radiol Clin North Am* 2001;39:1115-1135
17. Kimura S, Ashizawa K, Matsuyama N, Kadota J, Kohno S, Hayashi K. [Imaging of Wegener's granulomatosis: changes by serial chest CT]. *Nihon Kokyuki Gakkai Zasshi* 2002;40:171-176
18. Wong JS, Weisbrod GL, Chamberlain D, Herman SJ. Bronchioloalveolar carcinoma and the air bronchogram sign: a new pathologic explanation. *J Thorac Imaging* 1994;9:141-144
19. Kui M, Templeton PA, White CS, Cai ZL, Bai YX, Cai YQ. Evaluation of the air bronchogram sign on CT in solitary pulmonary lesions. *J Comput Assist Tomogr* 1996;20:983-986
20. Lee YR, Choi YW, Lee KJ, Jeon SC, Park CK, Heo JN. CT halo sign: the spectrum of pulmonary diseases. *Br J Radiol* 2005;78:862-865
21. Benamore RE, Weisbrod GL, Hwang DM, Bailey DJ, Pierre AF, Lazar NM, et al. Reversed halo sign in lymphomatoid granulomatosis. *Br J Radiol* 2007;80:e162-166